

Received 6 May 2021

Accepted 17 May 2021

Edited by L. Van Meervelt, Katholieke Universiteit Leuven, Belgium

Keywords: crystal structure; dihydroquinoxaline; hydrogen bond; π -stacking; C—H \cdots π (ring).

CCDC reference: 2062956

Supporting information: this article has supporting information at journals.iucr.org/e

Crystal structure and Hirshfeld surface analysis of 2-(2-oxo-3-phenyl-1,2,3,8a-tetrahydroquinoxalin-1-yl)ethyl acetate

Nadeem Abad,^{a,b} Houssaine El Ghayati,^c Camille Kalonji Mubengayi,^{d*} El Mokhtar Essassi,^c Savaş Kaya,^e Joel T. Mague^f and Youssef Ramli^{a*}

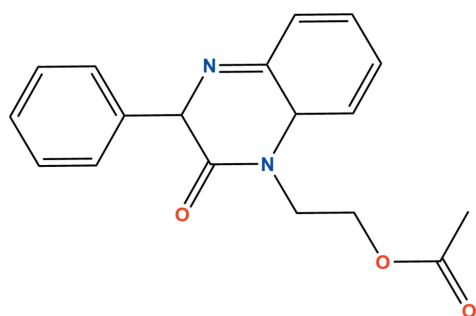
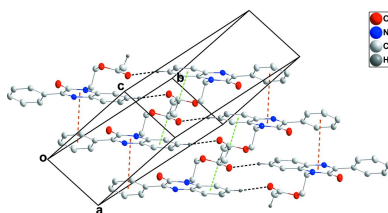
^aLaboratory of Medicinal Chemistry, Drug Sciences Research Center, Faculty of Medicine and Pharmacy, Mohammed V University in Rabat, Morocco, ^bDepartment of Biochemistry, Faculty of Education & Science, Al-Baydha University, Yemen, ^cLaboratoire de Chimie Organique Hétérocyclique, Faculté des Sciences, Université Mohammed V in Rabat, Morocco, ^dLaboratoire de Chimie et Biochimie de l'Institut Supérieur des Techniques Médicales de Kinshasa, République Démocratique du Congo, ^eSivas Cumhuriyet University, Health Services Vocational School, Department of Pharmacy, 58140, Sivas, Turkey, and ^fDepartment of Chemistry, Tulane University, New Orleans, LA 70118, USA.

*Correspondence e-mail: camillekalonji1@gmail.com, y.ramli@um5s.net.ma

In the title molecule, $C_{18}H_{16}N_2O_3$, the dihydroquinoxaline moiety, with the exception of the N atom is essentially planar with the inner part of the methylpropanoate group ($CH_2—CH_2—O$) nearly perpendicular to it. In the crystal, inversion dimers formed by C—H \cdots O hydrogen bonds are connected into oblique stacks by π -stacking and C—H \cdots π (ring) interactions.

1. Chemical context

Quinoxaline are a class of nitrogen containing heterocyclic compounds, found in many biologically active drugs (Ramli & Essassi, 2015; Ramli *et al.*, 2014). In addition, this heterocyclic scaffold possess anticorrosion characteristics (El Ouali *et al.*, 2010; Zarrok *et al.*, 2012; Tazouti *et al.*, 2016; El Aoufir *et al.*, 2016; Laabassi *et al.*, 2019). In a continuation of our recent work focused on the synthesis and biological evaluation of novel heterocyclic compounds (Guerrab *et al.* 2019, 2020, 2021; Abad *et al.*, 2021a,b; Missiou *et al.* 2021) we report here the crystal structure of the title compound (Fig. 1). As with many biologically active molecules, the molecular conformation adopted may have a significant effect on its activity.



2. Structural commentary

The dihydroquinoxaline moiety, with the exception of N1, is planar to within 0.0186 (9) Å (r.m.s. deviation of the nine fitted atoms = 0.0116 Å). N1 lies 0.0526 (12) Å below the



OPEN ACCESS

Table 1
Hydrogen-bond geometry (\AA , $^\circ$).

C_2 is the centroid of the C1–C6 benzene ring.

$D-\text{H}\cdots A$	$D-\text{H}$	$\text{H}\cdots A$	$D\cdots A$	$D-\text{H}\cdots A$
$\text{C}4-\text{H}4\cdots\text{O}3^{\text{i}}$	0.974 (16)	2.526 (16)	3.4713 (17)	163.6 (11)
$\text{C}5-\text{H}5\cdots\text{O}3$	0.992 (15)	2.592 (16)	3.5435 (15)	160.7 (12)
$\text{C}14-\text{H}14\cdots\text{O}1$	0.963 (15)	2.232 (16)	2.8387 (16)	120.0 (12)
$\text{C}16-\text{H}16B\cdots\text{O}3^{\text{ii}}$	0.993 (14)	2.553 (14)	3.3632 (16)	138.7 (10)
$\text{C}18-\text{H}18A\cdots C_2^{\text{iii}}$	0.97 (2)	2.93 (2)	3.7585 (17)	144.2 (17)

Symmetry codes: (i) $-x + 2, -y + 1, -z + 1$; (ii) $x - 1, y, z$; (iii) $-x + 1, -y + 1, -z + 1$.

mean plane. The C9–C14 phenyl ring is inclined to the above plane by $11.64 (6)^\circ$ while the inner part ($\text{CH}_2-\text{CH}_2-\text{O}$) of the methyl propanoate substituent is nearly perpendicular to the dihydroquinoxaline unit, as indicated by the angle of $87.34 (6)^\circ$ between the N1/C15/C16/O2 and N2/C1–C8 planes. The overall conformation is determined in part by the intramolecular $\text{C}5-\text{H}5\cdots\text{O}3$ and $\text{C}14-\text{H}14\cdots\text{O}1$ hydrogen bonds (Table 1 and Fig. 1).

3. Supramolecular features

In the crystal, inversion dimers are formed by $\text{C}4-\text{H}4\cdots\text{O}3$ hydrogen bonds [Table 1; symmetry code: (i) $-x + 2, -y + 1, -z + 1$] and are connected into oblique stacks by a combination of π -stacking interactions between the C1/C6/N1/C7/C8/N2 and C9–C14 rings [centroid–centroid distance = $3.7786 (9) \text{\AA}$, dihedral angle = $12.20 (6)^\circ$] and in addition $\text{C}16-\text{H}16B\cdots\text{O}3^{\text{ii}}$ and $\text{C}18-\text{H}18A\cdots C_2^{\text{iii}}$ interactions [Table 1 and Fig. 2; C_2 is the centroid of the C1–C6 ring; symmetry codes: (ii) $x - 1, y, z$, (iii) $-x + 1, -y + 1, -z + 1$]. The crystal packing also shows a $\text{C}17=\text{O}3\cdots C_2$ interaction [$\text{O}3\cdots C_2 = 3.9578 (12) \text{\AA}$, $\text{C}17\cdots C_2 = 3.7440 (16) \text{\AA}$, $\text{C}17=\text{O}3\cdots C_2 = 71.04 (8)^\circ$].

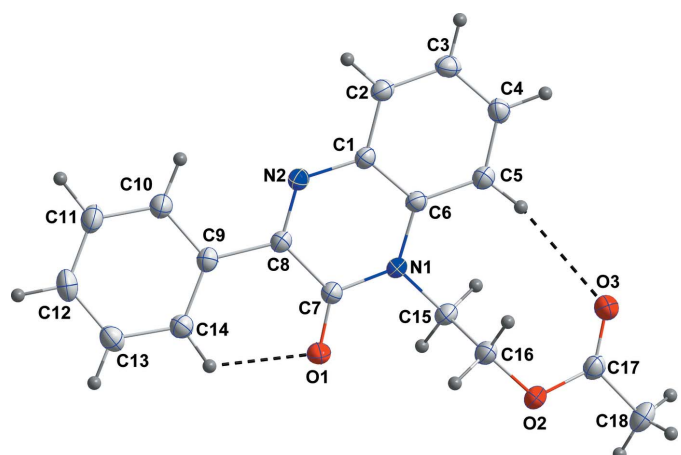


Figure 1

The title molecule with labelling scheme and 50% probability ellipsoids. The intramolecular $\text{C}-\text{H}\cdots\text{O}$ hydrogen bonds are shown by dashed lines.

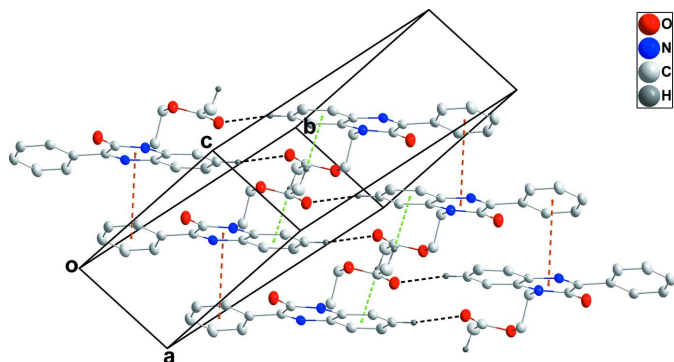
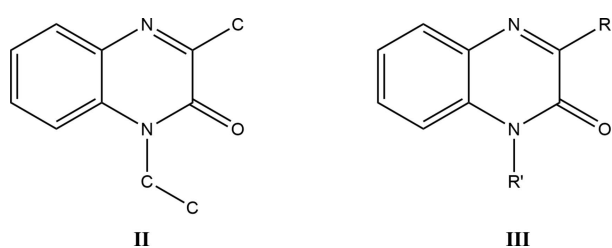


Figure 2

Perspective view of the packing. Intermolecular $\text{C}-\text{H}\cdots\text{O}$ hydrogen bonds are shown by black dashed lines while π -stacking and $\text{C}-\cdots\pi(\text{ring})$ interactions are shown, respectively, by orange and green dashed lines.

4. Database survey

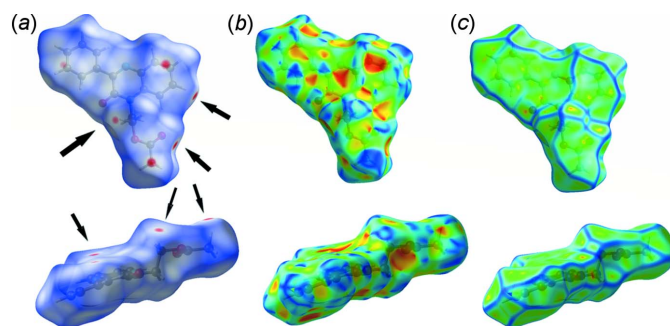
A survey of the Cambridge Structural Database (Version 5.42, last update February 2021; Groom *et al.*, 2016) using the search fragment **II** yielded 30 hits of which those most similar to the title molecule have the formula **III** with $R = \text{Me}$ and $R' = \text{CH}_2\text{CO}_2\text{H}$ (DEZJAW; Missioui *et al.*, 2018), $\text{CH}_2\equiv\text{CH}$ (DUCYUW; Benzeid *et al.*, 2009a), benzyl [DUSHUV (Ramli *et al.*, 2010b) and DUSHUV01 (Ramli *et al.*, 2018)], Et (IGANOU; Benzeid *et al.*, 2008), $\text{CH}_2\text{CH}=\text{CH}_2$ (YUPXAJ; Ramli *et al.*, 2010a), with $R = \text{CF}_3$ and $R' = i\text{-Bu}$ (DUBPUO; Wei *et al.*, 2019), with $R = \text{Ph}$ and $R' = \text{CH}_2(\text{cyclo-CHCH}_2\text{O})$ (NIBXEE; Abad *et al.*, 2018a), benzyl (PUGGII; Benzeid *et al.*, 2009b), $\text{CH}_2\text{CH}_2\text{CH}_2\text{OH}$ (RIRBOM; Abad *et al.*, 2018b), $\text{CH}_2\text{CO}_2\text{Et}$ (XEXWIJ; Abad *et al.*, 2018c), $\text{CH}_2\text{CH}=\text{CH}_2$ (YAJGEX; Benzeid *et al.*, 2011) and with $R = 3\text{-NO}_2\text{-C}_6\text{H}_4$ and $R' = \text{benzyl}$ (XIKHAD; Das *et al.*, 2018).



In the majority of the hits, the dihydroquinoxaline ring is essentially planar with the dihedral angle between the constituent rings being less than 1° or having the nitrogen bearing the exocyclic substituent less than 0.03\AA from the mean plane of the remaining nine atoms. Two notable exceptions are DEZJAW, where the dihedral angle between the two rings is 3.32° , and RIRBOM, where the nitrogen bearing the exocyclic substituent deviates by 0.062\AA from the plane defined by the other nine atoms.

5. Hirshfeld surface analysis

An effective means of probing intermolecular interactions is Hirshfeld surface analysis (McKinnon *et al.*, 2007; Spackman

**Figure 3**

Front (top) and side (bottom) views of the Hirshfeld surface plotted over (a) d_{norm} , (b) shape-index and (c) curvature.

& Jayatilaka, 2009), which can be conveniently carried out with *Crystal Explorer 17* (Turner *et al.*, 2017). A detailed description of the use of *Crystal Explorer 17* and the plots obtained has been published (Tan *et al.*, 2019) and will not be given here. Fig. 3a presents front (top) and side (bottom) views of the Hirshfeld surface plotted over d_{norm} in the range -0.1367 to 1.2965 a.u. One of the intramolecular C–H···O hydrogen bonds is indicated by the arrow at the left in the front view while those leading to the formation of the inversion dimers are shown by the arrows on the right of the front view. The C–H···π(ring) interaction and the π-stacking interactions are represented by the red spots designated by arrows in the side view. Fig. 3b presents the same two views of the surface plotted over the shape-index. In the front view, the π-stacking interaction is evident at the center as an orange triangle surrounded by blue triangles. Fig. 3c has the same two views of the surface plotted over the curvature index, with the flat area in the center indicating the locus of the π-stacking interaction. Fig. 4 presents fingerprint plots for all intermolecular interactions (a) and those delineated into H···H contacts (b, 49.4%), H···O/O···H contacts (c, 18.2%), H···C/C···H contacts (d, 17.8%) and C···C contacts (e, 7.2%).

6. Synthesis and crystallization

To a solution of 2-oxo-3-phenyl-1,2-dihydroquinoxaline (0.5 g, 2.25 mmol) in *N,N*-dimethylformamide (15 ml) were added 2-bromoethyl acetate (0.4 ml, 2.25 mmol), potassium carbonate (0.31 g, 2.25 mmol) and a catalytic quantity of tetra-*n*-butylammonium bromide. The reaction mixture was stirred at room temperature for 24 h. The solution was filtered and the solvent removed under reduced pressure. The residue thus obtained was chromatographed on a silica gel column using a hexane/ethyl acetate 9.5: 0.5 mixture as eluent. The solid obtained was recrystallized from ethanol solution to afford colorless column-like specimen of the title compound. Yield: 0.50 g, 67%; m.p. 471–473 K.

^1H NMR (Bruker Avance 300 MHz, CDCl_3) δ (ppm): 8.24 (*d*, 2H, Ar–H); 7.91 (*d*, 1H, Ar–H); 7.82 (*m*, 3H, Ar–H); 7.53 (*m*, 1H, Ar–H); 7.25 (*m*, 2H, Ar–H); 4.73 (*t*, 2H, O– CH_2); 3.92 (*t*, 2H, N– CH_2); 2.23 (*s*, 3H, OCOCH_3).

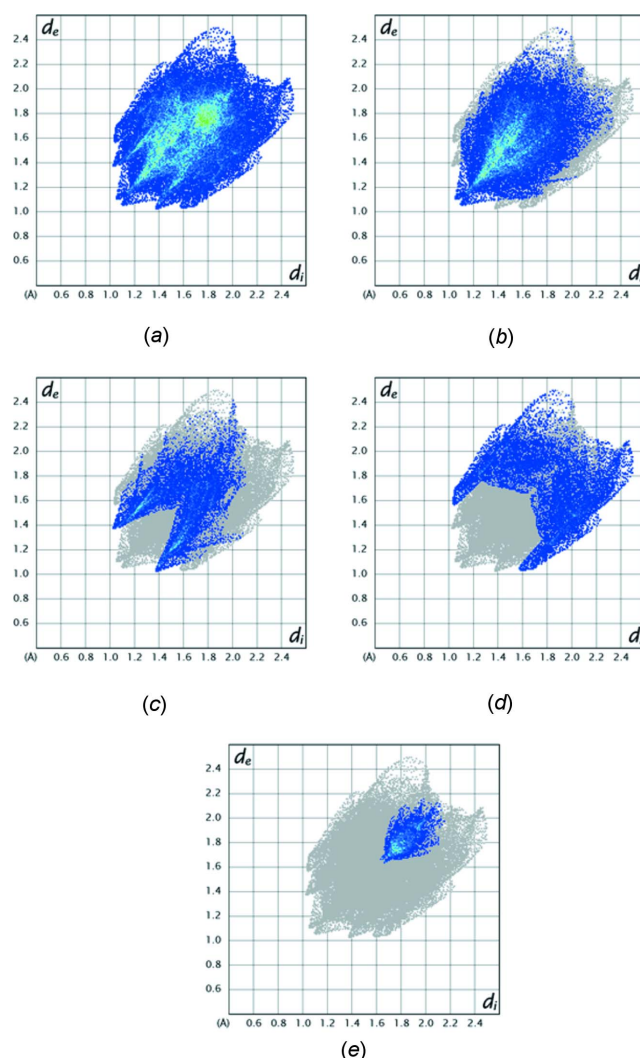
^{13}C NMR (Bruker Avance 75 MHz, CDCl_3) δ (ppm): 46.15 (N– CH_2); 61.15 (O– CH_2); 114.38, 123.82, 127.01, 127.72, 128.13, 128.96, 129.68, 130.33, 130.45, 130.62 (CH–Ar); 132.78, 133.36, 135.40, 136.05, 154.24 (Cq); 156.92 (C=O); 177.82 (O=C=O).

7. Refinement

Crystal data, data collection and structure refinement details are summarized in Table 2. All hydrogen atoms were located from a difference electron-density map and freely refined.

Acknowledgements

JTM thanks Tulane University for support of the Tulane Crystallography Laboratory. Author contributions are as follows. Conceptualization, YR and EME; synthesis, NA and LEG; writing (review and editing of the manuscript) CKM, JTM and YR; formal analysis, SK and JTM; crystal-structure determination, JTM; validation, JTM and YR, project administration, YR

**Figure 4**

Two dimensional fingerprint plots showing (a) all intermolecular interactions and those delineated into (b) H···H, (c) H···O/O···H, (d) H···C/C···H and (e) C···C interactions.

Table 2
Experimental details.

Crystal data	
Chemical formula	C ₁₈ H ₁₆ N ₂ O ₃
M _r	308.33
Crystal system, space group	Triclinic, P <bar>1</bar>
Temperature (K)	120
a, b, c (Å)	5.3518 (6), 11.6989 (14), 13.3527 (16)
α, β, γ (°)	64.019 (2), 80.323 (2), 76.952 (2)
V (Å ³)	729.83 (15)
Z	2
Radiation type	Mo K α
μ (mm ⁻¹)	0.10
Crystal size (mm)	0.42 × 0.18 × 0.12
Data collection	
Diffractometer	Bruker SMART APEX CCD
Absorption correction	Multi-scan (<i>SADABS</i> ; Krause <i>et al.</i> , 2015)
T _{min} , T _{max}	0.87, 0.99
No. of measured, independent and observed [I > 2σ(I)] reflections	14193, 3909, 2929
R _{int}	0.028
(sin θ/λ) _{max} (Å ⁻¹)	0.688
Refinement	
R[F ² > 2σ(F ²)], wR(F ²), S	0.049, 0.142, 1.00
No. of reflections	3909
No. of parameters	272
H-atom treatment	All H-atom parameters refined
Δρ _{max} , Δρ _{min} (e Å ⁻³)	0.47, -0.23

Computer programs: *APEX3* and *SAINT* (Bruker, 2016), *SHELXT* (Sheldrick, 2015a), *SHELXL2018/1* (Sheldrick, 2015b), *DIAMOND* (Brandenburg & Putz, 2012) and *SHELXTL* (Sheldrick, 2008).

References

- Abad, N., Ferfra, S., Essassi, E. M., Mague, J. T. & Ramli, Y. (2021b). *Z. Kristallogr. New Cryst. Struct.* **236**, 173–175.
- Abad, N., El Bakri, Y., Sebhaoui, J., Ramli, Y., Essassi, E. M. & Mague, J. T. (2018a). *IUCrData*, **3**, x180610.
- Abad, N., El Bakri, Y., Sebhaoui, J., Ramli, Y., Essassi, E. M. & Mague, J. T. (2018c). *IUCrData*, **3**, x180519.
- Abad, N., Ramli, Y., Lahmudi, S., El Hafi, Y., Essassi, E. M. & Mague, J. T. (2018b). *IUCrData*, **3**, x181633.
- Abad, N., Sallam, H. H., Al-Ostoot, F. H., Khamees, H. A., Al-horaibi, S. A., Khanum, S. A., Madegowda, M., Hafi, M. E., Mague, J. T., Essassi, E. M. & Ramli, Y. (2021a). *J. Mol. Struct.* **1232**, 130004.
- Benzeid, H., Bouhfid, R., Massip, S., Leger, J. M. & Essassi, E. M. (2011). *Acta Cryst. E67*, o2990.
- Benzeid, H., Ramli, Y., Vendier, L., Essassi, E. M. & Ng, S. W. (2009a). *Acta Cryst. E65*, o2196.
- Benzeid, H., Saffon, N., Garrigues, B., Essassi, E. M. & Ng, S. W. (2009b). *Acta Cryst. E65*, o2685.
- Benzeid, H., Vendier, L., Ramli, Y., Garrigues, B. & Essassi, E. M. (2008). *Acta Cryst. E64*, o2234.
- Brandenburg, K. & Putz, H. (2012). *DIAMOND*, Crystal Impact GbR, Bonn, Germany.
- Bruker (2016). *APEx3, SADABS* and *SAINT*. Bruker AXS Inc., Madison, Wisconsin, USA.
- Das, D. K., Pampana, V. K. K. & Hwang, K. C. (2018). *Chem. Sci.* **9**, 7318–7326.
- El Aoufir, Y., Lgaz, H., Bourazmi, H., Kerroum, Y., Ramli, Y., Guenbour, A., Salghi, R., El-Hajjaji, F., Hammouti, B. & Oudda, H. (2016). *J. Mater. Environ. Sci.* **7**, 4330–4347.
- El Ouali, I., Hammouti, B., Aouniti, A., Ramli, Y., Azougagh, M., Essassi, E. M. & Bouachrine, M. (2010). *J. Mater. Envir. Sci.* **1**, 1–8.
- Groom, C. R., Bruno, I. J., Lightfoot, M. P. & Ward, S. C. (2016). *Acta Cryst. B72*, 171–179.
- Guerrab, W., Chung, I.-M., Kansiz, S., Mague, J. T., Dege, N., Taoufik, J., Salghi, R., Ali, I. H., Chung, I. M., Lgaz, H. & Ramli, Y. (2019). *J. Mol. Struct.* **1197**, 127630.
- Guerrab, W., Lgaz, H., Kansiz, S., Mague, J. T., Dege, N., Ansar, M., Marzouki, R., Taoufik, J., Ali, I. H., Chung, I. M. & Ramli, Y. (2020). *J. Mol. Struct.* **1205**, 127630.
- Guerrab, W., Missiou, M., Zaoui, Y., Mague, J. T. & Ramli, Y. (2021). *Z. Kristallogr. New Cryst. Struct.* **236**, 133–134.
- Krause, L., Herbst-Irmer, R., Sheldrick, G. M. & Stalke, D. (2015). *J. Appl. Cryst.* **48**, 3–10.
- Laabaisi, T., Benhiba, F., Rouifi, Z., Allali, M., Missiou, M., Ourrak, K., Oudda, H., Ramli, Y., Warad, I. & Zarrouk, A. (2019). *Int. J. Corros. Scale Inhib.* **8**, 241–256.
- McKinnon, J. J., Jayatilaka, D. & Spackman, M. A. (2007). *Chem. Commun.* pp. 3814–3816.
- Missiou, M., El Fal, M., Taoufik, J., Essassi, E. M., Mague, J. T. & Ramli, Y. (2018). *IUCrData*, **3**, x180882.
- Missiou, M., Mortada, S., Guerrab, W., Serdaroglu, G., Kaya, S., Mague, J. T., Essassi, E. M., Faouzi, M. E. A. & Ramli, Y. (2021). *J. Mol. Struct.* In the press.
- Ramli, Y., El Bakri, Y., El Ghayati, L., Essassi, E. M. & Mague, J. T. (2018). *IUCrData*, **3**, x180390.
- Ramli, Y. & Essassi, E. M. (2015). *Adv. Chem. Res.* **27**, 109–160.
- Ramli, Y., Moussaif, A., Karrouchi, K. & Essassi, E. M. (2014). *J. Chem.* Article ID 563406, 1–21.
- Ramli, Y., Moussaif, A., Zouihri, H., Lazar, S. & Essassi, E. M. (2010b). *Acta Cryst. E66*, o1922.
- Ramli, Y., Slimani, R., Zouihri, H., Lazar, S. & Essassi, E. M. (2010a). *Acta Cryst. E66*, o1767.
- Sheldrick, G. M. (2008). *Acta Cryst. A64*, 112–122.
- Sheldrick, G. M. (2015a). *Acta Cryst. A71*, 3–8.
- Sheldrick, G. M. (2015b). *Acta Cryst. C71*, 3–8.
- Spackman, M. A. & Jayatilaka, D. (2009). *CrystEngComm*, **11**, 19–32.
- Tan, S. L., Jotani, M. M. & Tiekkink, E. R. T. (2019). *Acta Cryst. E75*, 308–318.
- Tazouti, A., Galai, M., Touir, R., Touhami, M. E., Zarrouk, A., Ramli, Y., Saracoğlu, M., Kaya, S., Kandemirli, F. & Kaya, C. (2016). *J. Mol. Liq.* **221**, 815–832.
- Turner, M. J., McKinnon, J. J., Wolff, S. K., Grimwood, D. J., Spackman, P. R., Jayatilaka, D. & Spackman, M. A. (2017). *Crystal Explorer 17*. The University of Western Australia.
- Wei, Z., Qi, S., Xu, Y., Liu, H., Wu, J., Li, H., Xia, C. & Duan, G. (2019). *Adv. Synth. Catal.* **361**, 5490–5498.
- Zarrok, H., Zarrouk, A., Salghi, R., Oudda, H., Hammouti, B., Ebn Touhami, M., Bouachrine, M. & Pucci, O. H. (2012). *Electrochim. Acta*, **30**, 405–417.

supporting information

Acta Cryst. (2021). E77, 643-646 [https://doi.org/10.1107/S2056989021005247]

Crystal structure and Hirshfeld surface analysis of 2-(2-oxo-3-phenyl-1,2,3,8a-tetrahydroquinoxalin-1-yl)ethyl acetate

Nadeem Abad, Lhoussaine El Ghayati, Camille Kalonji Mubengayi, El Mokhtar Essassi, Savaş Kaya, Joel T. Mague and Youssef Ramli

Computing details

Data collection: *APEX3* (Bruker, 2016); cell refinement: *SAINT* (Bruker, 2016); data reduction: *SAINT* (Bruker, 2016); program(s) used to solve structure: *SHELXT* (Sheldrick, 2015*a*); program(s) used to refine structure: *SHELXL2018/1* (Sheldrick, 2015*b*); molecular graphics: *DIAMOND* (Brandenburg & Putz, 2012); software used to prepare material for publication: *SHELXTL* (Sheldrick, 2008).

2-(2-Oxo-3-phenyl-1,2,3,8a-tetrahydroquinoxalin-1-yl)ethyl acetate

Crystal data

$C_{18}H_{16}N_2O_3$	$Z = 2$
$M_r = 308.33$	$F(000) = 324$
Triclinic, $P\bar{1}$	$D_x = 1.403 \text{ Mg m}^{-3}$
$a = 5.3518 (6) \text{ \AA}$	$Mo K\alpha$ radiation, $\lambda = 0.71073 \text{ \AA}$
$b = 11.6989 (14) \text{ \AA}$	Cell parameters from 5207 reflections
$c = 13.3527 (16) \text{ \AA}$	$\theta = 3.1\text{--}29.3^\circ$
$\alpha = 64.019 (2)^\circ$	$\mu = 0.10 \text{ mm}^{-1}$
$\beta = 80.323 (2)^\circ$	$T = 120 \text{ K}$
$\gamma = 76.952 (2)^\circ$	Column, colourless
$V = 729.83 (15) \text{ \AA}^3$	$0.42 \times 0.18 \times 0.12 \text{ mm}$

Data collection

Bruker SMART APEX CCD	14193 measured reflections
diffractometer	3909 independent reflections
Radiation source: fine-focus sealed tube	2929 reflections with $I > 2\sigma(I)$
Graphite monochromator	$R_{\text{int}} = 0.028$
Detector resolution: 8.3333 pixels mm^{-1}	$\theta_{\max} = 29.3^\circ, \theta_{\min} = 1.7^\circ$
φ and ω scans	$h = -7 \rightarrow 7$
Absorption correction: multi-scan	$k = -16 \rightarrow 16$
(<i>SADABS</i> ; Krause <i>et al.</i> , 2015)	$l = -18 \rightarrow 18$
$T_{\min} = 0.87, T_{\max} = 0.99$	

Refinement

Refinement on F^2	272 parameters
Least-squares matrix: full	0 restraints
$R[F^2 > 2\sigma(F^2)] = 0.049$	Primary atom site location: structure-invariant
$wR(F^2) = 0.142$	direct methods
$S = 1.00$	Secondary atom site location: difference Fourier
3909 reflections	map

Hydrogen site location: difference Fourier map
 All H-atom parameters refined
 $w = 1/[\sigma^2(F_o^2) + (0.0999P)^2]$
 where $P = (F_o^2 + 2F_c^2)/3$

$(\Delta/\sigma)_{\max} < 0.001$
 $\Delta\rho_{\max} = 0.47 \text{ e } \text{\AA}^{-3}$
 $\Delta\rho_{\min} = -0.23 \text{ e } \text{\AA}^{-3}$

Special details

Experimental. The diffraction data were obtained from 3 sets of 400 frames, each of width 0.5° in ω , collected at $\varphi = 0.00, 90.00$ and 180.00° and 2 sets of 800 frames, each of width 0.45° in φ , collected at $\omega = -30.00$ and 210.00° . The scan time was 30 sec/frame.

Geometry. All esds (except the esd in the dihedral angle between two l.s. planes) are estimated using the full covariance matrix. The cell esds are taken into account individually in the estimation of esds in distances, angles and torsion angles; correlations between esds in cell parameters are only used when they are defined by crystal symmetry. An approximate (isotropic) treatment of cell esds is used for estimating esds involving l.s. planes.

Refinement. Refinement of F^2 against ALL reflections. The weighted R-factor wR and goodness of fit S are based on F^2 , conventional R-factors R are based on F, with F set to zero for negative F^2 . The threshold expression of $F^2 > 2\text{sigma}(F^2)$ is used only for calculating R-factors(gt) etc. and is not relevant to the choice of reflections for refinement. R-factors based on F^2 are statistically about twice as large as those based on F, and R-factors based on ALL data will be even larger.

Fractional atomic coordinates and isotropic or equivalent isotropic displacement parameters (\AA^2)

	x	y	z	$U_{\text{iso}}^*/U_{\text{eq}}$
O1	0.24048 (17)	0.11347 (8)	0.45539 (7)	0.0287 (2)
O2	0.42582 (17)	0.24290 (8)	0.68691 (6)	0.0264 (2)
O3	0.74296 (17)	0.36037 (9)	0.62940 (7)	0.0308 (2)
N1	0.52749 (18)	0.24890 (9)	0.40271 (7)	0.0209 (2)
N2	0.46952 (18)	0.31557 (9)	0.18053 (7)	0.0205 (2)
C1	0.6193 (2)	0.37704 (11)	0.20843 (9)	0.0198 (2)
C2	0.7488 (2)	0.47088 (11)	0.12307 (9)	0.0229 (3)
H2	0.731 (3)	0.4919 (13)	0.0454 (12)	0.033 (4)*
C3	0.9057 (2)	0.53135 (11)	0.14791 (10)	0.0253 (3)
H3	0.999 (3)	0.5940 (13)	0.0898 (11)	0.025 (3)*
C4	0.9332 (2)	0.50106 (12)	0.25984 (10)	0.0240 (3)
H4	1.043 (3)	0.5462 (13)	0.2757 (11)	0.023 (3)*
C5	0.8070 (2)	0.40967 (11)	0.34551 (10)	0.0229 (3)
H5	0.835 (3)	0.3898 (15)	0.4234 (13)	0.035 (4)*
C6	0.6527 (2)	0.34508 (11)	0.32082 (9)	0.0197 (2)
C7	0.3624 (2)	0.19025 (11)	0.37929 (9)	0.0209 (2)
C8	0.3496 (2)	0.22703 (11)	0.25807 (9)	0.0193 (2)
C9	0.2018 (2)	0.16113 (11)	0.22093 (9)	0.0210 (2)
C10	0.2376 (3)	0.18294 (12)	0.10782 (10)	0.0268 (3)
H10	0.365 (3)	0.2385 (15)	0.0602 (13)	0.040 (4)*
C11	0.1007 (3)	0.12852 (13)	0.06609 (10)	0.0307 (3)
H11	0.131 (3)	0.1475 (15)	-0.0164 (14)	0.045 (4)*
C12	-0.0746 (3)	0.05042 (12)	0.13563 (11)	0.0299 (3)
H12	-0.174 (3)	0.0113 (13)	0.1067 (11)	0.026 (3)*
C13	-0.1069 (2)	0.02574 (12)	0.24773 (11)	0.0282 (3)
H13	-0.229 (3)	-0.0255 (14)	0.2925 (12)	0.030 (4)*
C14	0.0284 (2)	0.08023 (11)	0.29077 (10)	0.0239 (3)
H14	-0.004 (3)	0.0579 (14)	0.3697 (12)	0.030 (4)*

C15	0.5682 (2)	0.20405 (12)	0.52109 (9)	0.0224 (3)
H15A	0.751 (3)	0.2084 (12)	0.5233 (10)	0.019 (3)*
H15B	0.546 (2)	0.1157 (14)	0.5606 (11)	0.023 (3)*
C16	0.3790 (2)	0.28659 (12)	0.57099 (9)	0.0246 (3)
H16A	0.388 (3)	0.3773 (14)	0.5287 (11)	0.027 (3)*
H16B	0.200 (3)	0.2750 (12)	0.5718 (10)	0.024 (3)*
C17	0.6177 (2)	0.28800 (12)	0.70394 (10)	0.0246 (3)
C18	0.6508 (3)	0.23944 (15)	0.82550 (11)	0.0319 (3)
H18A	0.545 (4)	0.305 (2)	0.8477 (19)	0.085 (7)*
H18B	0.600 (4)	0.1579 (19)	0.8692 (16)	0.063 (5)*
H18C	0.829 (4)	0.2289 (18)	0.8386 (15)	0.060 (5)*

Atomic displacement parameters (\AA^2)

	U^{11}	U^{22}	U^{33}	U^{12}	U^{13}	U^{23}
O1	0.0367 (5)	0.0329 (5)	0.0186 (4)	-0.0178 (4)	0.0010 (3)	-0.0080 (4)
O2	0.0315 (5)	0.0335 (5)	0.0192 (4)	-0.0123 (4)	0.0016 (3)	-0.0136 (4)
O3	0.0309 (5)	0.0397 (5)	0.0282 (4)	-0.0145 (4)	0.0022 (4)	-0.0175 (4)
N1	0.0248 (5)	0.0241 (5)	0.0160 (4)	-0.0082 (4)	0.0008 (4)	-0.0094 (4)
N2	0.0230 (5)	0.0203 (5)	0.0195 (4)	-0.0044 (4)	-0.0001 (4)	-0.0097 (4)
C1	0.0212 (5)	0.0209 (5)	0.0188 (5)	-0.0040 (4)	0.0007 (4)	-0.0102 (4)
C2	0.0267 (6)	0.0224 (6)	0.0191 (5)	-0.0050 (5)	0.0012 (4)	-0.0089 (4)
C3	0.0282 (6)	0.0221 (6)	0.0236 (6)	-0.0081 (5)	0.0039 (5)	-0.0080 (5)
C4	0.0239 (6)	0.0247 (6)	0.0280 (6)	-0.0063 (5)	-0.0005 (4)	-0.0147 (5)
C5	0.0241 (6)	0.0256 (6)	0.0220 (5)	-0.0051 (4)	-0.0004 (4)	-0.0127 (5)
C6	0.0203 (5)	0.0205 (5)	0.0185 (5)	-0.0043 (4)	0.0017 (4)	-0.0091 (4)
C7	0.0237 (6)	0.0216 (5)	0.0191 (5)	-0.0063 (4)	0.0002 (4)	-0.0097 (4)
C8	0.0209 (5)	0.0201 (5)	0.0178 (5)	-0.0029 (4)	-0.0013 (4)	-0.0092 (4)
C9	0.0225 (6)	0.0200 (5)	0.0217 (5)	-0.0020 (4)	-0.0038 (4)	-0.0097 (4)
C10	0.0338 (7)	0.0276 (6)	0.0223 (5)	-0.0105 (5)	-0.0018 (5)	-0.0110 (5)
C11	0.0415 (7)	0.0316 (7)	0.0246 (6)	-0.0096 (5)	-0.0061 (5)	-0.0141 (5)
C12	0.0322 (7)	0.0285 (6)	0.0373 (7)	-0.0059 (5)	-0.0088 (5)	-0.0188 (6)
C13	0.0266 (6)	0.0269 (6)	0.0337 (6)	-0.0085 (5)	-0.0009 (5)	-0.0137 (5)
C14	0.0235 (6)	0.0243 (6)	0.0246 (6)	-0.0049 (4)	-0.0009 (4)	-0.0109 (5)
C15	0.0265 (6)	0.0247 (6)	0.0170 (5)	-0.0068 (5)	-0.0007 (4)	-0.0089 (4)
C16	0.0254 (6)	0.0309 (6)	0.0202 (5)	-0.0069 (5)	-0.0011 (4)	-0.0122 (5)
C17	0.0245 (6)	0.0294 (6)	0.0241 (5)	-0.0037 (5)	-0.0003 (4)	-0.0161 (5)
C18	0.0388 (8)	0.0373 (8)	0.0229 (6)	-0.0034 (6)	-0.0053 (5)	-0.0159 (6)

Geometric parameters (\AA , $^\circ$)

O1—C7	1.2275 (13)	C9—C14	1.3995 (16)
O2—C17	1.3467 (14)	C9—C10	1.4036 (15)
O2—C16	1.4489 (13)	C10—C11	1.3828 (17)
O3—C17	1.2043 (14)	C10—H10	0.990 (16)
N1—C7	1.3800 (14)	C11—C12	1.3884 (19)
N1—C6	1.3882 (14)	C11—H11	1.016 (16)
N1—C15	1.4692 (13)	C12—C13	1.3822 (18)

N2—C8	1.3016 (14)	C12—H12	0.988 (14)
N2—C1	1.3763 (14)	C13—C14	1.3894 (17)
C1—C2	1.4022 (15)	C13—H13	0.934 (15)
C1—C6	1.4114 (14)	C14—H14	0.962 (14)
C2—C3	1.3721 (17)	C15—C16	1.5155 (17)
C2—H2	0.972 (15)	C15—H15A	0.996 (13)
C3—C4	1.4027 (16)	C15—H15B	0.958 (14)
C3—H3	0.962 (13)	C16—H16A	0.967 (14)
C4—C5	1.3795 (16)	C16—H16B	0.993 (14)
C4—H4	0.973 (14)	C17—C18	1.4940 (16)
C5—C6	1.3975 (16)	C18—H18A	0.97 (2)
C5—H5	0.992 (15)	C18—H18B	0.95 (2)
C7—C8	1.4911 (14)	C18—H18C	0.97 (2)
C8—C9	1.4861 (15)		
C17—O2—C16	115.33 (9)	C9—C10—H10	117.0 (9)
C7—N1—C6	123.19 (9)	C10—C11—C12	120.53 (12)
C7—N1—C15	116.52 (9)	C10—C11—H11	118.3 (9)
C6—N1—C15	120.28 (9)	C12—C11—H11	121.2 (9)
C8—N2—C1	120.49 (9)	C13—C12—C11	119.10 (11)
N2—C1—C2	119.20 (9)	C13—C12—H12	119.6 (8)
N2—C1—C6	121.67 (10)	C11—C12—H12	121.3 (8)
C2—C1—C6	119.10 (10)	C12—C13—C14	121.02 (12)
C3—C2—C1	120.73 (10)	C12—C13—H13	117.5 (9)
C3—C2—H2	119.6 (8)	C14—C13—H13	121.4 (9)
C1—C2—H2	119.7 (8)	C13—C14—C9	120.32 (11)
C2—C3—C4	119.78 (11)	C13—C14—H14	116.0 (9)
C2—C3—H3	121.2 (8)	C9—C14—H14	123.7 (9)
C4—C3—H3	119.0 (8)	N1—C15—C16	110.08 (9)
C5—C4—C3	120.72 (11)	N1—C15—H15A	106.2 (7)
C5—C4—H4	120.7 (8)	C16—C15—H15A	112.9 (7)
C3—C4—H4	118.5 (8)	N1—C15—H15B	109.3 (8)
C4—C5—C6	119.78 (10)	C16—C15—H15B	110.1 (8)
C4—C5—H5	118.0 (9)	H15A—C15—H15B	108.2 (11)
C6—C5—H5	122.2 (9)	O2—C16—C15	109.30 (10)
N1—C6—C5	122.87 (9)	O2—C16—H16A	111.5 (8)
N1—C6—C1	117.29 (10)	C15—C16—H16A	111.6 (8)
C5—C6—C1	119.84 (10)	O2—C16—H16B	105.9 (7)
O1—C7—N1	120.36 (10)	C15—C16—H16B	110.3 (7)
O1—C7—C8	124.70 (10)	H16A—C16—H16B	108.0 (11)
N1—C7—C8	114.94 (9)	O3—C17—O2	123.41 (10)
N2—C8—C9	117.09 (9)	O3—C17—C18	124.81 (11)
N2—C8—C7	122.12 (10)	O2—C17—C18	111.77 (10)
C9—C8—C7	120.78 (9)	C17—C18—H18A	104.9 (13)
C14—C9—C10	118.14 (10)	C17—C18—H18B	113.1 (11)
C14—C9—C8	124.43 (10)	H18A—C18—H18B	110.9 (18)
C10—C9—C8	117.43 (10)	C17—C18—H18C	111.5 (11)
C11—C10—C9	120.87 (11)	H18A—C18—H18C	110.2 (17)

C11—C10—H10	122.2 (9)	H18B—C18—H18C	106.3 (16)
C8—N2—C1—C2	179.20 (10)	O1—C7—C8—N2	175.20 (11)
C8—N2—C1—C6	1.29 (17)	N1—C7—C8—N2	-5.32 (16)
N2—C1—C2—C3	-178.09 (10)	O1—C7—C8—C9	-6.07 (18)
C6—C1—C2—C3	-0.13 (17)	N1—C7—C8—C9	173.42 (9)
C1—C2—C3—C4	-1.29 (18)	N2—C8—C9—C14	-168.77 (10)
C2—C3—C4—C5	0.91 (18)	C7—C8—C9—C14	12.44 (17)
C3—C4—C5—C6	0.92 (18)	N2—C8—C9—C10	10.61 (16)
C7—N1—C6—C5	175.87 (10)	C7—C8—C9—C10	-168.19 (10)
C15—N1—C6—C5	-4.42 (16)	C14—C9—C10—C11	1.58 (18)
C7—N1—C6—C1	-4.13 (16)	C8—C9—C10—C11	-177.84 (11)
C15—N1—C6—C1	175.58 (10)	C9—C10—C11—C12	-0.4 (2)
C4—C5—C6—N1	177.66 (10)	C10—C11—C12—C13	-1.2 (2)
C4—C5—C6—C1	-2.34 (17)	C11—C12—C13—C14	1.52 (19)
N2—C1—C6—N1	-0.14 (16)	C12—C13—C14—C9	-0.28 (19)
C2—C1—C6—N1	-178.05 (10)	C10—C9—C14—C13	-1.26 (17)
N2—C1—C6—C5	179.86 (10)	C8—C9—C14—C13	178.11 (10)
C2—C1—C6—C5	1.95 (16)	C7—N1—C15—C16	-92.28 (12)
C6—N1—C7—O1	-173.92 (10)	C6—N1—C15—C16	88.00 (12)
C15—N1—C7—O1	6.36 (16)	C17—O2—C16—C15	82.16 (12)
C6—N1—C7—C8	6.57 (15)	N1—C15—C16—O2	-178.70 (9)
C15—N1—C7—C8	-173.15 (9)	C16—O2—C17—O3	0.52 (16)
C1—N2—C8—C9	-177.24 (9)	C16—O2—C17—C18	179.37 (10)
C1—N2—C8—C7	1.54 (17)		

Hydrogen-bond geometry (\AA , $^\circ$)

Cg2 is the centroid of the C1—C6 benzene ring.

$D\text{—H}\cdots A$	$D\text{—H}$	$H\cdots A$	$D\cdots A$	$D\text{—H}\cdots A$
C4—H4 \cdots O3 ⁱ	0.974 (16)	2.526 (16)	3.4713 (17)	163.6 (11)
C5—H5 \cdots O3	0.992 (15)	2.592 (16)	3.5435 (15)	160.7 (12)
C14—H14 \cdots O1	0.963 (15)	2.232 (16)	2.8387 (16)	120.0 (12)
C16—H16B \cdots O3 ⁱⁱ	0.993 (14)	2.553 (14)	3.3632 (16)	138.7 (10)
C18—H18A \cdots Cg2 ⁱⁱⁱ	0.97 (2)	2.93 (2)	3.7585 (17)	144.2 (17)

Symmetry codes: (i) $-x+2, -y+1, -z+1$; (ii) $x-1, y, z$; (iii) $-x+1, -y+1, -z+1$.